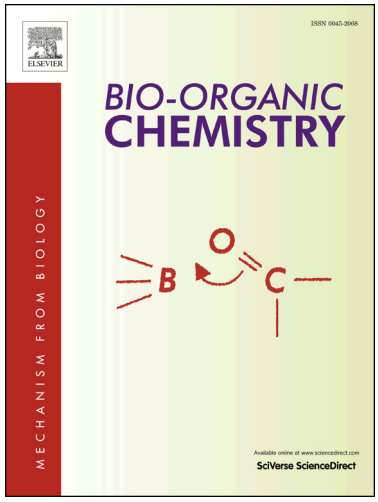

Novel Quinuclidinone Derivatives Induced Apoptosis in Human Breast Cancer *via* Targeting P53

Ahmed Malki, Rasha Y. Elbayaa, Omnia Ali, Ahmed Sultan, Amal M. Youssef

PII: S0045-2068(16)30415-1
DOI: http://dx.doi.org/10.1016/j.bioorg.2017.03.010
Reference: YBIOO 2037

To appear in: *Bioorganic Chemistry*

Received Date: 17 December 2016
Revised Date: 7 March 2017
Accepted Date: 21 March 2017

Please cite this article as: A. Malki, R.Y. Elbayaa, O. Ali, A. Sultan, A.M. Youssef, Novel Quinuclidinone Derivatives Induced Apoptosis in Human Breast Cancer *via* Targeting P53, *Bioorganic Chemistry* (2017), doi: http://dx.doi.org/10.1016/j.bioorg.2017.03.010

Novel Quinuclidinone Derivatives Induced Apoptosis in Human Breast Cancer *via* Targeting P53

Ahmed Malki[a, *], Rasha Y. Elbayaa[b, c], Omnia Ali[d], Ahmed Sultan[d], Amal M. Youssef [b, e, *]

[a]Department of Biomedical Science, College of Health Sciences, Qatar University, Doha, Qatar.

[b]Department of Pharmaceutical Chemistry, Faculty of Pharmacy, Alexandria University, Alexandria, Egypt.

[c]Department of Analytical & Pharmaceutical Chemistry, Faculty of Pharmacy & Drug Manufacturing , Pharos University in Alexandria, 21311, Egypt.

[d]Department of Biochemistry, Faculty of Science, Alexandria University, Alexandria, Egypt.

[e]College of Pharmacy, Al Ain University of Science and Technology, Al Ain, United Arab Emirates.

*Dr Ahmed Malki, Department of Biomedical Science, College of Health Sciences, Qatar University, Doha, Qatar ahmed.malki@qu.edu.qa., permanent address Biochemistry department, Faculty of Science, Alexandria University, Alexandria, Egypt.

*Correspondence: Prof. Amal Youssef, College of Pharmacy, Al Ain University of Science and Technology, P.O. Box: 64141, Al Ain, United Arab Emirates. Tel: +971 3 7024873; Fax: +971 3 7024777. E-mail: ayoussef65@yahoo.com

Keywords

Synthesis; Quinuclidinone; p53; Breast Cancer; Apoptosis; Docking.

Abstract

Small molecules that can target human cancers have been highly sought to increase the anticancer efficacy, the present work describes the design and synthesis of novel series of five quinuclidinone derivatives **(2a-2e)**. Their anticancer activities were investigated against breast cancer cells MCF-7, MDA-MB-231 breast cancer cells harboring mutant p53 and normal breast counterpart MCF-12a. Derivative **2e** reduced proliferation of MCF-7 and MCF-12a while it has no effect on MDA-MB-231. Derivative **2e** induced apoptosis in MCF-7 cells which is further confirmed by TUNEL assay and it reduced the percentage of cell in G2/M phase as confirmed by increased expression of cyclin B and reduced expression of cyclin D1. Derivative **2e** reduced expression levels of Mdm2, Akt and ERK1/2 by and increased expression level of p53. Moreover, the apoptosis induction by **2e** was also inhibited by PFT-α as evidenced by non-significant induction of apoptosis after treatment of MCF-7 cells with both derivative **2e** and PFT-α. In addition, docking study reveals that derivative **2e** has a binding pattern close to the pattern observed in the structure of the lead fragment 5,6-dimethoxy-2-methylbenzothiazole bound to T-p53C-Y220C. The above findings demonstrate that derivative **2e** induces apoptosis in MCF-7 cells via targeting p53 which merits further development.

1. Introduction

Cancer today accounts for more deaths worldwide than tuberculosis, HIV, and malaria combined. Breast cancer is the most common cancer among women. It will afflict an estimated 9.1 million women in poorer countries over the next decade. Of the 5 million women expected to die from breast cancer in the next decade, 70 percent will live in low- and middle-income countries[1].

Breast cancer is a heterogeneous disease and different breast cancer subtypes can be identified based on gene expression profiling. Current breast cancer therapies, based on Selective Estrogen Receptor Modulators (SERMs), such as tamoxifen or aromatase inhibitors, can be unsuccessful due to intrinsic or acquired resistance to these therapies[2]. Consequently, discovery and development of new class of anticancer drugs are urgently needed to combat the growing threat of high mortality rate.

Quinuclidinones belongs to the group of bicyclic bridgehead lactams and are highly twisted. This twisted nature decreases the delocalization effect, increasing the basicity of the nitrogen so that it often behaves more like an amine than as a typical planar amide. This might increase selectivity and affinity of a pharmacophore element towards different receptor binding sites[3]. Literature survey revealed that The molecule 3-quinuclidinone is an attractive candidate in medicinal chemistry as it constitute the building block of wide range of many pharmacologically active compounds having anticancer effect[4], antihistamine-bronchodilating activity[5], nicotinic receptors inhibitory activity[6], anti Alzheimer's effect[7]. In addition, it has been reported that quinuclidine moiety constitute the basic skeleton for many synthetic pharmacologically active existing drugs for example; palonosetron and azasetron as 5-HT3 receptor blockers[8], solifenacin and cevimeline as muscarinic receptor antagonists[9], and quinupramine as a tricyclic antidepressant[10] (Figure 1).

Moreover, in a previous publication - in our laboratoy - quinuclidinone demonstrated an excellent scaffold for novel anti-cancer agents with improved safety profile. With the intact carbonyl group of quinuclidinone, more potent derivatives against lung carcinoma cells were reported[11]. In addition, novel quinuclidinone analogs that induce cytotoxicity in human non-small lung carcinoma cell line (H1299) null for p53, a tumor suppressor protein, have previously been reported[12]. In continuation on our research program, it was also confirmed that other quinuclidinone derivatives induce apoptosis in human breast cancer cells via reduced expression level of Bcl-2,Bcl-XL and increased mitochondrial apoptotic pathways by activating the release of cytochrome C[13]. The conventional view of p53-mediated

apoptosis has emphasized its role as a transcription factor[14]. The p53 protein been thought to be the molecular target of Pifithrin-alpha (PFT) which has been widely used as a ubiquitous and reversible inhibitor of p53 and p53 mediated apoptosis[15]. The pharmacological rescue of inactive p53 may therefore represent an attractive therapeutic strategy. Pifithrin-alpha (PFT) is an inhibitor of p53 and is considered to be useful for therapeutic suppression to protect against various genotoxic agents [16]. Several reports have shown that Pifithrin-alpha (PFT) blocks the p53-mediated activation of autophagy caused by stress-inducing agents 17. PFT has been validated as a useful p53 inhibitor for the elucidation of p53 functions in experimental studies.The pharmacological salvage of inactive p53 may represent an attractive therapeutic tool. Pifithrin-alpha (PFT) is an inhibitor of p53 and is considered to be useful for therapeutic suppression in order to reduce cancer treatment side effects and to protect against various genotoxic agents[16]. Several reports have shown that PFT blocks the p53-mediated apoptotic effect caused by chemical agents[17]. In summary, PFT has been validated as a useful p53 inhibitor for investigating p53 functions in experimental studies.

In view of the above mentioned results and as a continuation of our research on Quinuclidinones in an attempt to identify new lead compounds that might be of value for future development as new class of anticancer agents, a series of novel quinuclidinone based amines **(2a-2e)** were synthesized. The structures of title compounds were well supported by spectroscopic data and elemental analysis. The target compounds comprise some pharmacophoric elements which influence the biological activity of the molecules, such as the aryl ring as hydrophobic binding site, the nitrogen of the secondary amine as electron donor, additional NH group as hydrogen bonding domain. To understand the mechanism of action and the effects on cancer biology, we evaluated the effect of the most promising compounds on cell cycle, apoptosis and the tumor suppressor p53. A molecular docking study was also performed for the most active compounds in a trial to investigate the possible mode of action of these compounds.

2. Results and discussion

2.1. Chemistry

The synthetic strategies to obtain the target compounds are depicted in Scheme 1. The key starting material 2-methylenequinuclidine-3-one hydrochloride **1** was refluxed with phenyl and 4-nitrophenyl hydrazine in ethanol in the presence of sodium bicarbonate to yield the corresponding *N*-[(3-oxo-quinuclidin-2yl)methyl]-*N*'-phenylhydrazine **2a** and

N-[(3-oxo-quinuclidin-2yl)methyl]-*N*'-4-nitrophenylhydrazine **2b**, respectively. Reacting the starting compound **1** with different amines in the presence of sodium bicarbonate yielded secondary amine substituted 2-methylenequinuclidine-3-one namely; 2-[(4-chloroanilino)methyl]-3-quinuclidone **2c**[18], 2-[(4-bromoanilino)methyl]-3-quinuclidone **2d**[18], and 2-[(1*H*-benzo[*d*]imidazol-2-ylamino)methyl]-3-quinuclidone **2e**. The synthesized compounds were supported by spectroscopic data. The ^{1}H-NMR (ppm) of the resulted compounds were characterized by the presence of multiplet allocated for $NCHCH_2$, doublet or multiplet for the aromatic ring-Hs, multiplet for the benzimidazole $C_{4,7}$-Hs, multiplet for the benzimidazole $C_{5,6}$-Hs at the expected range of δ –ppm scale and a D_2O exchangeable singlet for the NH.

Biological evaluation

2.2.1. Quinuclidinone derivatives 2e reduced cell proliferation and induced apoptosis in breast cancer cells

Previously our laboratory reported novel quinuclidinone derivatives which reduced proliferation of lung cancer cell lines. In this report, we managed to synthesize and confirm structures of these derivatives **(2a-2e)**. We investigated the effect of the proposed five quinuclidinone derivatives against breast cancer cells MCF-7 and MDA-MB-231 to determine if the potent derivative is working in p53 dependent or independent mechanism. We first showed the impact of these 5 derivatives on proliferations of breast cancer cells (MCF-7 and MDA-MB-231). Our data indicated that 10 µM quinuclidinone derivatives **2e** was potent in decreasing cell viability in MCF-7 breast cancer cells (20%) compared to control untreated cells (Figure2A). The dose response curve was constructed to determine IC50 for the potent derivative **2e** (Figure 2B). We used 4 µM of derivative **2e** and also examined its cytotoxcity against normal breast epithelial cells (MCF-12a) and results are represented in Figure2C. To determine if the decreased cells viability is linked to apoptosis, ELISA assay was performed to detect histone release from apoptotic cells, revealing that 4µM of **2e** treatment induced apoptosis in MCF-7 cells compared with non-treated control ($P<0.05$) (Figure2D). The results were confirmed by immunohistochemical analysis using TUNEL assay which showed the formation of more TUNEL positive cells in MCF-7 up on treatment of cells with derivative **2e** (Figure2E).

We treated MDA-MB-231 with derivative **2e** in order to determine if this derivative is working via p53 dependent or p53 independent mechanism. Our data revealed that our

derivatives **2e** did not affects the cell viability in MDA-MB-231 cells and it did not induce any significant increase in apoptosis under the same conditions (Figure 2F,G).

2.2.2. Quinuclidinone derivatives 2e modulates G2/M checkpoint

MCF-7 cells were treated with 4 μM of **2e** and harvested after 24 h and showed a significant decrease in the percent of G2/M cells (10%) compared to control group (30%) (Figure 3A). The abrogation of G2/M checkpoint was confirmed by the increased expression levels of cyclin B (2-fold increase) and reduction of cyclin D levels (4-fold decrease) (Figure 3B).

2.2.3. Quinuclidinone derivatives 2e modifies apoptotic signals and increase p53 expression

Apoptosis occurs due to an imbalance between pro and anti-apoptotic proteins. Derivative **2e** reduced expression levels of Mdm2, Akt and ERK1/2 by (4, 3 and 2 fold respectively) and increased expression level of p53 (2.5-fold) (Figure 4A). We next examined the role of p53 transcription by using a p53 transcriptional inhibitor, PFT-α, a specific inhibitor of p53 transcriptional targets. As shown in Figure3A, PFT-α inhibited the up-regulation of p53 and it suppressed activation of p53 targets Mdm2, Akt and Erk1/2 (Figure 4B). Moreover, the apoptosis induction by **2e** was also inhibited by PFT-α as evidenced by non-significant induction of apoptosis after treatment of MCF-7 cells with both **2e** and PFT-α (Figure 4C).

From the above study it was appeared that compound **2e** is the most active deivative. It induced apoptosis in MCF-7 and increasesd expression of tumor suppressor p53. The increased activity of compound **2e** is related to the pharmacophoric elements which influence its biological activity such as NH group of benzimidazole ring which forms an additional hydrogen bonding domain. In addition, benzimidazole ring displayed hydrophobic interactions with the hydrophobic binding site in the receptor.

2.2. Molecular Modeling

The docking study was carried out using the enzyme parameters obtained from the crystallographic structure of T-p53C-Y220C (a stable variant of p53 core domain with the Y220C mutation) bound to the lead fragment 5,6-dimethoxy-2-methylbenzothiazole

(PDB ID: 2X0W)[19]. The docking simulation for the ligand was carried out using molecular operating environment (MOE) software supplied by the Chemical Computing Group, Inc., Montréal Canada[20].

The structure of lead fragment 5,6-dimethoxy-2-methylbenzothiazole bound to T-p53C-Y220C showed that the molecule sits in an upright position within the mutation-induced cavity (Figure5). The thiazole nitrogen is within hydrogen-bonding distance of the hydroxyl group of Thr150. The methoxy moieties of the molecule sit at the bottom of the cavity in close proximity to Cys220.

Figure 6 shows the binding mode of compound **2e** docked and minimized in the mutation induced cavity of T-p53C-Y220C. In this case, hydrogen bond is observed between the nitrogen of benzimidazole and the hydroxyl group of Thr150. Hydrogen bond is also observed between NH group and oxygen of Thr150.
In addition, compound **2e** displayed hydrophobic interactions with the same amino acids Val147, Pro151, Cys 220 and Glu221 bound to the lead fragment.

The docking study shows that compound **2e** has a binding pattern which is close to the pattern observed in the structure of the lead fragment 5,6-dimethoxy-2-methylbenzothiazole bound to T-p53C-Y220C. Compound **2e** forms hydrogen bonds with the same residue (Thr150) as that observed in the structure of the lead fragment with T-p53C-Y220C. This may account for increased activity recorded for compound **2e**.

3. Conclusion

Apoptosis occurs due to an imbalance between pro and anti-apoptotic proteins. Derivative **2e** reduced proliferation and induced apoptosis in MCF-7 cells with no impact on MDA-MB-231. The tumor suppressor p53 exerts its biological effect by regulating transcription of numerous downstream target genes involved in cell cycle arrest, apoptosis and DNA repair, In order to better understand the mechanisms of action of compounds that target mutant p53, it is important to determine whether they can directly bind with mutant p53 or proteins involved in the process of mutant p53 reactivation or depletion. Additionally, it reduced expression levels of Mdm2, Akt and ERK1/2 and increased expression level of p53. We next examined the role of p53 transcription by using a p53 transcriptional inhibitor, PFT-α, a specific inhibitor of

p53 transcriptional targets. PFT-α inhibited the up-regulation of p53 and it suppressed activation of p53 targets Mdm2, Akt and Erk1/2. Moreover, the apoptosis induction by derivative **2e** was also inhibited by PFT-α as evidenced by non-significant induction of apoptosis after treatment of MCF-7 cells with both **2e** and PFT-α. Additionally, derivative **2e** forms hydrogen bonds with the same residue (Thr150) as that observed in the structure of the lead fragment with T-p53C-Y220C. This may account for increased expression levels of p53 recorded for derivative **2e**. Our results suggest that derivative **2e** might be promising anticancer agent in breast cancer cells via targeting p53.

4. Experimental

4.1. Chemistry

Melting points were determined in open-glass capillaries on SMP10–Barloworld Scientific melting point apparatus and are uncorrected. The infrared (IR) spectra were recorded on Perkin-Elmer 1430 infrared spectrophotometer using the KBr palate technique. ^{1}H spectra were run on a Varian spectrometer (300 MHz), Faculty of Science, Cairo University using tetramethylsilane (TMS) as the internal standard and DMSO-d_6 as the solvent (Chemical shifts in δ, ppm). Splitting patterns were designated as follows: s: singlet; d: doublet; t: triplet; q: quartet and m: multiplet. Microanalyses were performed at the at the Microanalytical unit, Faculty of Science, Cairo University and the found values were within ±0.4% of the theoretical values.

4.1.1. General procedure for preparation of compounds **2a-e**

A mixture of 2-methylenequinuclidine-3-one hydrochloride **1** (0.174 g, 0.001 mole), sodium bicarbonate (0.084 g, 0.001 mole) and phenyl hydrazine, 4-nitrophenyl hydrazine or the appropriate amine (0.001 mole) in ethanol (5 ml) was heated under reflux for 12-18 h. The solvent was evaporated under reduced pressure and the remaining solid was triturated with water, filtered, dried and crystallized from methanol.

4.1.1.1. N-[(3-Oxo-quinuclidin-2yl)methyl]-N'-phenylhydrazine **2a**

Yield: 80%, mp: 145-148 ^{o}C. IR (cm^{-1}): 3150, 3110 (NH); 1730 (C=O). ^{1}H-NMR (δ ppm):1.68-1.93 (m, 4H, 2 CH_2); 2.38 (bs, 1H, bridgehead); 2.62-2.82 (m, 4H, 2 NCH_2);

3.12-3.17 (m, 3H, $NCHCH_2$), 4.32 (s, 1H, NH, D_2O exchangeable); 7.01-7.49 (m, 5H, aromatic H). Anal.Calcd for $C_{14}H_{19}N_3O$ (245.32): C, 68.54; H, 7.81; N, 17.13. Found: C, 68.78; H, 8.05; N, 16.89.

4.1.1.2. N-[(3-oxo-quinuclidin-2yl)methyl]-N'-4-nitrophenylhydrazine **2b**

Yield: 88%, mp: 170-172 ^oC. IR (cm^{-1}): 3145, 3120 (NH); 1730 (C=O). ^1H-NMR (δ ppm):1.48-1.86 (m, 4H, 2 CH_2); 2.37 (bs, 1H, bridgehead); 2.57-2.78 (m, 4H, 2 NCH_2); 2.80-2.89 (m, 3H, $NCHCH_2$); 4.28 (s, 1H, NH, D_2O exchangeable); 7.36 (d, 2H, J = 8.5 Hz, aromatic H); 8.11 (d, 2H, J = 8.5 Hz, aromatic H). Anal.Calcd for $C_{14}H_{18}N_4O_3$ (290.32): C, 57.92; H, 6.25; N, 19.30. Found: C, 58.13; H, 6.41; N, 19.59.

4.1.1.3. 2-[(4-Chloroanilino)methyl]-3-quinuclidone **2c**

Yield: 80%, mp: 126-128 ^oC [reported 127-131 ^oC][18].

4.1.1.4. 2-[(4-Bromoanilino)methyl]-3-quinuclidone **2d**

Yield: 85%, mp: 131-135 ^oC [reported 132-134 ^oC][18].

4.1.1.5. 2-[(1*H*-Benzo[*d*]imidazol-2-ylamino)methyl]-3-quinuclidone **2e**

Yield: 86%, mp: 160-162 ^oC. IR (cm^{-1}): 3236, 3128 (NH); 1730 (C=O). ^1H-NMR (δ ppm):1.77-1.90 (m, 4H, 2 CH_2); 2.26 (bs, 1H, bridgehead); 2.70-2.91 (m, 4H, 2 NCH_2); 2.93-3.23 (m, 3H, $NCHCH_2$); 6.05 (s, 1H, NH, D_2O exchangeable); 6.79--6.81 (m, 2H, benzimidazole-$C_{5,6}$-H); 7.04-7.07 (m, 2H, benzimidazole-$C_{4,7}$-H). Anal.Calcd for $C_{15}H_{18}N_4O$ (270.33): C, 66.64; H, 6.71; N, 20.73. Found: C, 67.05; H, 6.84; N, 20.39.

4.2. Biological evaluation

4.2.1. Cell culture and Compound treatment

MCF-7, breast cancer cells with wild type p53 geneand MDA-MB-231 breast cells have a mutant p53 were purchased from ATCC (USA). MCF-7 cells were maintained in Dulbecco's modified essential media (DMEM) (Gibco, California, USA) supplemented with 10% Fetal Bovine Serum, 100 Units/ml penicillin and 100 µg/ml

streptomycin at 37^{o}C in a 5% CO2 atmosphere (Gibco, California, USA). MCF-12a cells were maintained in DMEM/F-12 media (Gibco, California, USA) supplemented with 10% FBS, 100 Units/mL penicillin, 100 µg/mL streptomycin, insulin (1.2 g/L), transferrin (0.001 mg/mL), EGF (20ng/µL) and hydrocortisone (500 ng/mL) at 37°C in a 5% CO_2 atmosphere. The synthesized compounds were prepared in 10µM concentration and dissolved in suitable media.PFTα (1-(4-methylphenyl)-2-(4,5,6,7-tetrahydro-2-imino-3(2H)benzothiazolyl)ethanone hydrobromide) was purchased from Cayman Chemical Company (Ann Arbor, Michigan USA).

4.2.2. Methyl tetrazolium (MTT) bromide mitochondrial activity assay

Cell viability was measured by MTT (3-(4,5-dimethylthiazol-2-yl)-2,5-diphenyltetrazolium bromide) assay as described previously(ATCC, Manassas, VA USA). Briefly, 4000- 5000 cells/well in 100 µL of medium were seeded into 96-well plates. After 24 h incubation at 37 °C, the culture media were removed and replaced with fresh media containing the test compounds (100 µM). The cells were incubated for another 24 h then, 10 µL of 5 mg/ mL MTT reagent was added to each well and incubated for 4 h at 37 °C. After incubation, 100 µL of detergent reagent was added to each well to dissolve the formazan crystals. The absorbance was determined at 570 nmusing Spectra Max Plus. Each assay was performed in triplicate and the experiment was repeated three times and standard deviation was determined. To determine the IC_{50} of compound **2e**, the assay was conducted using different concentrations of compound **2e** and the average 50% inhibitory concentration (IC_{50}) was determined from the dose response curve.

4.2.3. Enzyme linked immunosorbent apoptosis assay

Cells were seeded at a density of 2 X 10^4/ well in a 96- well plate and incubated for 24 hours. Media were changed to media containing compound **2e (**4 µM). Cells were then incubated for 24 hours. An ELISA assay was performed using Cell Death Detection ELISA^{PLUS} kit (Roche-Applied Science, Indianapolis, USA) that measures histone release from fragmented DNA in apoptosing cells. Briefly, cells were lysed with 200-µL lysis buffer for 30 min at room temperature. The lysate was centrifuged at 200 g for 10 min. 150 µL of supernatant was collected, of which 20 µL was incubated with anti-histone biotin and anti-DNA peroxidase at room temperature for 2 h. After washing with incubation buffer three times, 100 µL of substrate solution (2,2`azino-di(3-

ethylbenzthiazolin-sulphuric acid) was added to each well and incubated for 15-20 min at room temperature. The absorbance was measured using an ELISA reader (Spectra Max Plus) at 405 nm. Each assay was done in triplicate and the standard deviation was determined.

4.2.4. TUNEL assay

For in situ detection of apoptotic cells, TUNEL (terminal-deoxynucleotidyl transferase meditated nick end labeling) assay was performed using DeadEnd^{TM}fluorimetric tunnel system (Promega, USA). Cells were cultured on 4-chamber slides (VWR, USA) at a density of 2 X10^4 cells/ chamber. After treatment with 4μM of compound **2e**, cells were washed with phosphate buffer saline (PBS) and fixed by incubation in 4% paraformaldehyde (PFA) for 20 min at 4 ^oC, then permeabilized with 0.05% triton X-100 for 5 min at 4 ^oC. The fixed cells were then incubated with digoxigenin-conjugated dUTP in terminal deoxynucleotide transferase recombinant (rTdT)-catalyzed reaction and nucleotide mixture for 60 min at 37 ^oC in a humidified atmosphere and then immersed in stop/wash buffer for 15 min at room temperature. Cells were then washed with PBS to remove unincorporated fluorescein-12-dUTP. After washing with PBS, cells were incubated in 1μg/ml 2-(4-amidinophenyl)-6-indole carbamidinedihydrochloride (DAPI) and fluorescinisothiocyanate (FITC) solution for 15 min in dark (data not shown). Cells were observed with fluorescence microscopy (RT slider Spot, Diagnostic Instruments, Inc) and photographed at 100X magnification.

4.2.5. Cell cycle analysis

Cells were seeded at a density of 3-5 X 10^5/ 10 cm plateand incubated for 24 h before treatment. Media was changed to media containing 4 μM of compound **2e**, 24 hours later, cells were harvested by trypsinization. The cells were washed with PBS and fixed with ice-cold 70 % ethanol while vortexing. Finally, the cells were washed and resuspended in PBS containing 5 μg/mL RNase A (Sigma, St. Louis, MO USA) and 50 μg/mL propidium iodide (Sigma, St. Louis, MO USA) for analysis. Cell cycle analysis was performed using FACScan Flow Cytometer (Becton Dickson) according to the manufacturer's protocol. Windows multiple document interfaces (WinMDI) software was used to calculate the cell-cycle phase distribution from the resultant DNA histogram, and expressed as a percentage of cells in the G0/G1 and G2/M phases. The apoptotic cells were identified on the DNA histogram as a subdiploid peak.

4.2.6. Determination of pro-apoptotic, anti-apoptotic proteins by Western blotting analysis

Total protein was extracted from cells treated with 4 µM of compound **2e** and untreated cells using lysis buffer (10 mMTrisHCl pH 7.5, 1 mM EDTA, 1% triton X-100, 150 mMNaCl, 1 mMdithiothretol, 10% glycerol, 0.2 mMphenylmethysulphonyl fluoride and protease inhibitors) for 30-50 min on ice. The extracts were centrifuged at 13,000 rpm for 15 min at 4°C to remove cell debris. Folin Lowry (Pierce, USA) protein assay was used to determine the protein concentration in the cell lysates. Proteins were resolved by electrophoresis on 8-10% sodium dodecyl sulphate – polyacrylamide gel loading equal amount of proteins per lane. The resolved proteins were transferred to polyvinylidene difluoride (PVDF) membrane and then probed with primary antibody against the protein of interest prepared in 5% milk/PBS-T. The membrane was washed using Phosphate-buffered Saline with Tween 20 (PBS-T) and then appropriate secondary antibody conjugated to horseradish peroxidase (HRP) was used for visualization of the bands using ECL chemiluminescence kit (GE, USA). AntiP53 anti-Mdm2, anti-ERK1/2, anti- Akt, anti-cyclinD1 and anti-cyclin B were purchased from SantaCruz, USA. MEK1 and SP600125 were purchased from Santa cruz, USA. Pixel density of the proteins studied was calculated using Image J, version 1.41o, NIH. The obtained values were first normalized to loading control β-actin) and folds increase was measured by normalizing to the control (0 hr) value. At least two independent experiments were performed.

4.3. Molecular modeling studies

Computer-assisted simulated docking experiments were carried out under an MMFF94X forcefield using Molecular Operating Environment (MOE Dock 2009) software, Chemical Computing Group, Montréal, Canada.

The coordinates from the X-ray crystal structure of T-p53C-Y220C used in this simulation were obtained from the Protein Data Bank (PDB ID: 2X0W), where the active site is bound to 5,6-dimethoxy-2-methylbenzothiazole. The ligand molecule was constructed using the builder module and were energy minimized. The active site of T-p53C-Y220C was generated using the MOE-Alpha Site Finder, and then the ligand was docked within this active site using the MOE Dock. The lowest energy conformation

was selected and the ligand interactions (hydrogen bonding and hydrophobic interaction) with T-p53C-Y220C were determined.

5. Conflict of interest

The authors report no conflicts of interest. The authors alone are responsible for the contents and writing the paper.

Acknowledgements

The authors would like to thank the Department of Health Sciences, Qatar University for financial support of the cancer biology part of this work.

References

1. J. Poorolajal , N. Nafissi , M. E. Akbari , H. Mahjub , N. Esmailnasab, E. Babaee. Arch Iran Med. 19 (2016) 680-686.
2. R. Weinshilboum. Adv. Exp. Med. Biol. 630 (2008) 220–231.
3. T. Kousuke, M. S. Brian. Nature 441 (2006) 731-734.
4. J. Y. Soni, S. Sanghvi, R.V. Devkarb, S. Thakore. RSC Adv. 5 (2015) 82112-82120.
5. F. J. Villani, T. A. Mann, E. A.Wefer. J. Med. Chem. 18 (1975) 666–669.
6. H. R. Arias, J. J. López, D. Feuerbach, A. Fierro, M. O. Ortells, E. G. Pérez.Int. J. Biochem. Cell Biol. 45 (2013) 2420-2430.
7. M. I. Rodríguez-Franco, I. Dorronsoro, A. Castro, A. Martínez, A. Badía, J. E. Baños. Bioorg. Med. Chem. 11 (2003) 2263-2268.
8. C. Rojas, M. Stathis, A. G. Thomas, E. B. Massuda, J. Alt, J. Zhang, E. Rubenstein, S. Sebastiani, S. Cantoreggi, S. H. Snyder, B. Slusher. Anesth. Analg. 107 (2008) 469-478.
9. M. Ishii, Y .Kurachi. Curr. Pharm. Des. 12 (2006) 3573-3581.
10. P. K. Panegyres, E. Armari. Am. J. Neurodegener. Dis. 2 (2013) 176-186.
11. A. Malki, A. B. Pulipaka, S. C. Evans, S. C. Bergmeier. Bioorg. Med. Chem. Lett. 16 (2006) 1156-1159.
12. A. Malki, elS. El Ashry. J. Chemother. 24 **(**2012**)** 268-278.
13. A. Malki, elS. El Ashry**.** Anticancer Res. 34 (2014) 1367-1376.
14. K. H. Vousden, X. Lu. Nat. Rev. Cancer 2 (2002) 594-605.
15. F. J. Waters, T. Shavlakadze, M. J. McIldowie, M. J. Piggott, M. D. Grounds. Mol. Cell Biochem. 337 (2010) 119–131.
16. E. A. Komarova, A. V. Gudkov. Semin. Cancer Biol. 8 (1998) 389-400.

17. B. S . Zhu, C. G. Xing, F.Lin, X. Q. Fan, K. Zhao, Z. H. Qin. World J. Gastroenterol. 17 (2011) 478-487.
18. S. Elkin, H. Lieberman. U.S. patent (1973) 3, 726, 877.
19. N. Basse, J. L. Kaar, G. Settanni, A. C. Joerger, T. J. Rutherford, A. R. Fersht. Chem. Biol. 1 **(**2010**)** 746-56.
20. Molecular Operating Environment (MOE) 2009. 10, Chemical Computing Group Inc., 1010 Sherbrooke Street West, Suite 910, Montréal, H3A 2R7, Canada, http://www.chemcomp.com

List of figures

Figure 1

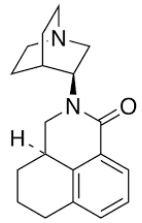

Palonosetron

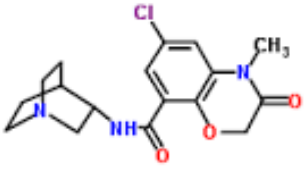

Azasetron

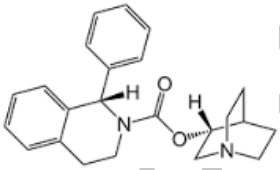

Solifencin

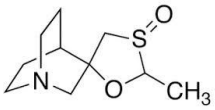

Cevimeline

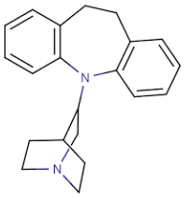

Quinupramine

Figure 2

A

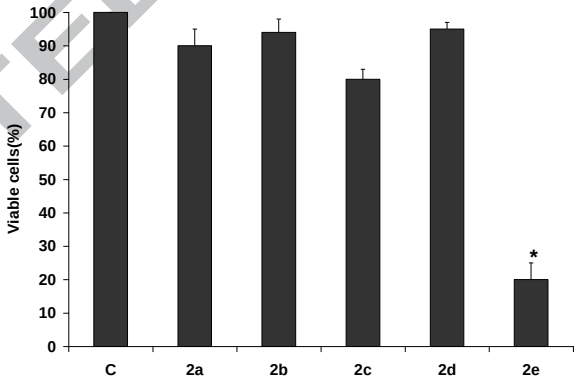

B

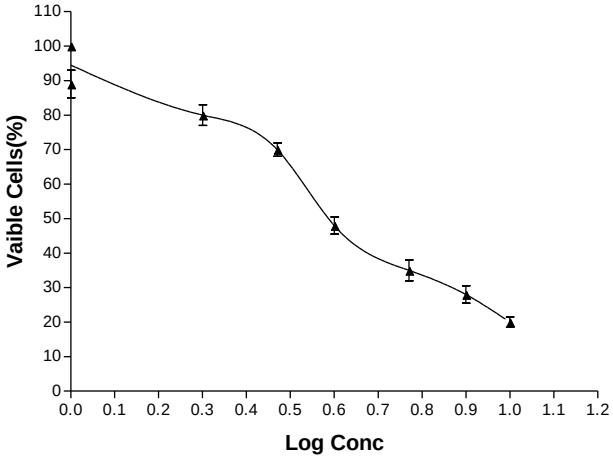

C

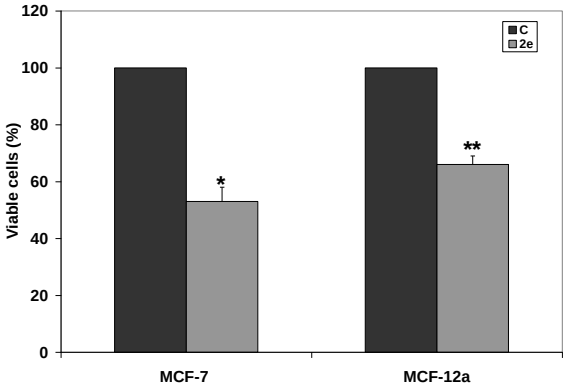

D

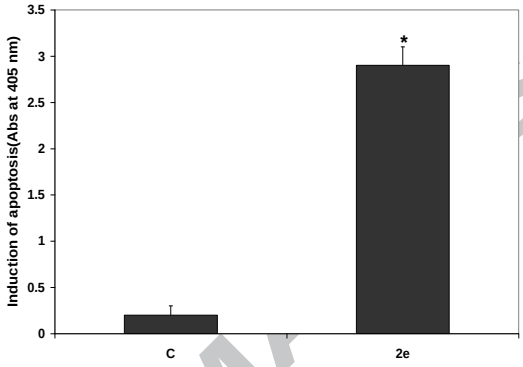

E

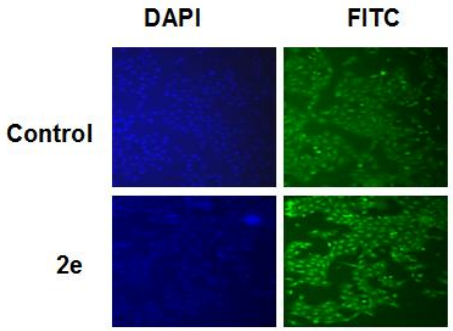

F

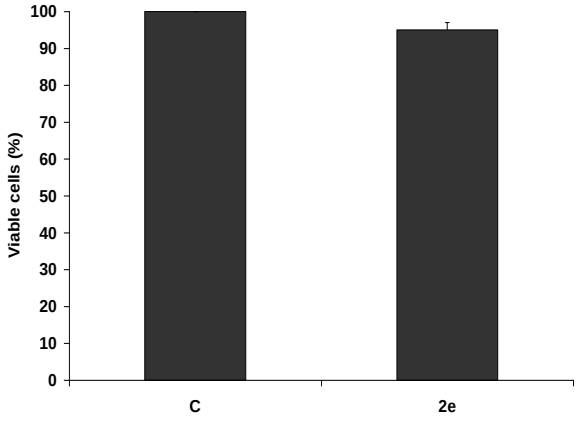

G

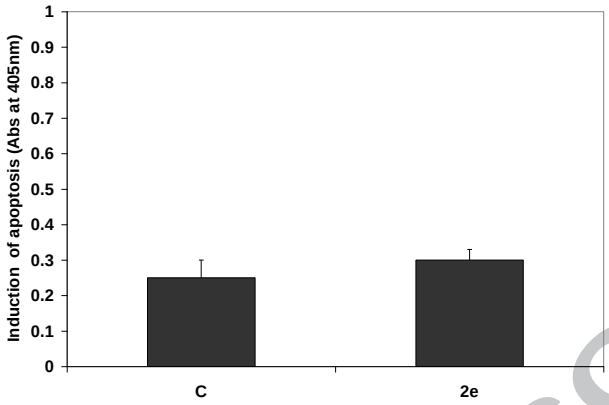

Figure 3

A

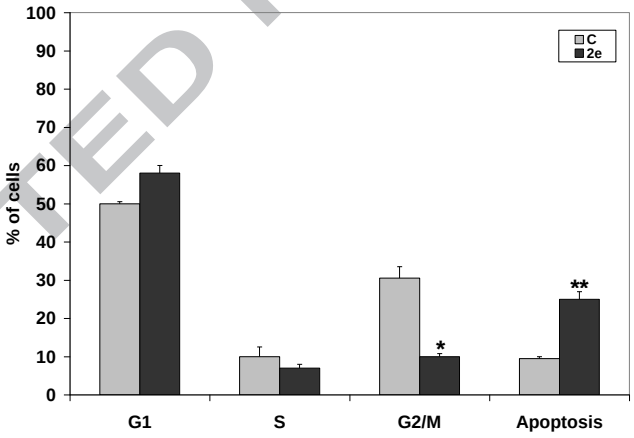

B

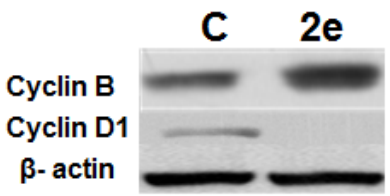

Figure 4

a

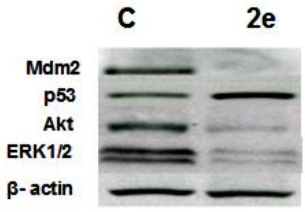

b

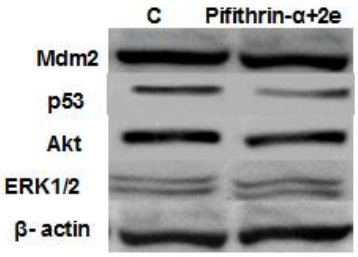

c

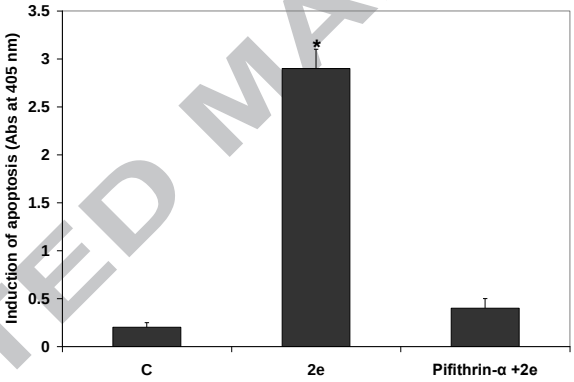

Figure 5

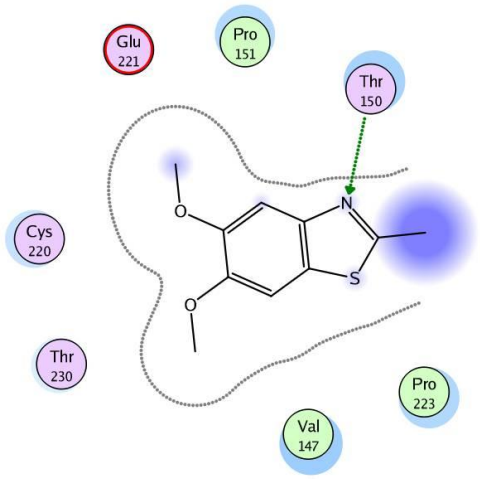

Figure 6

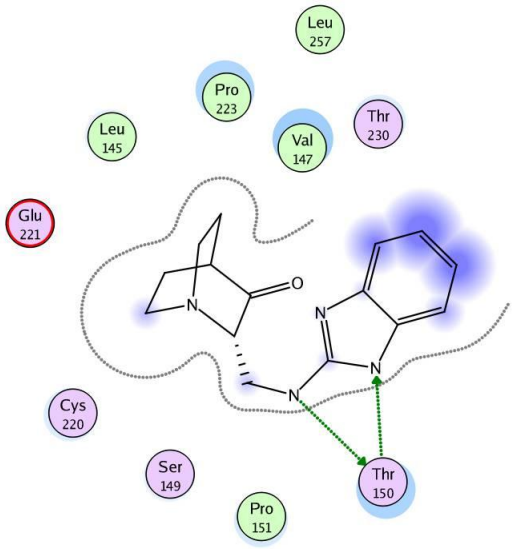

Scheme 1

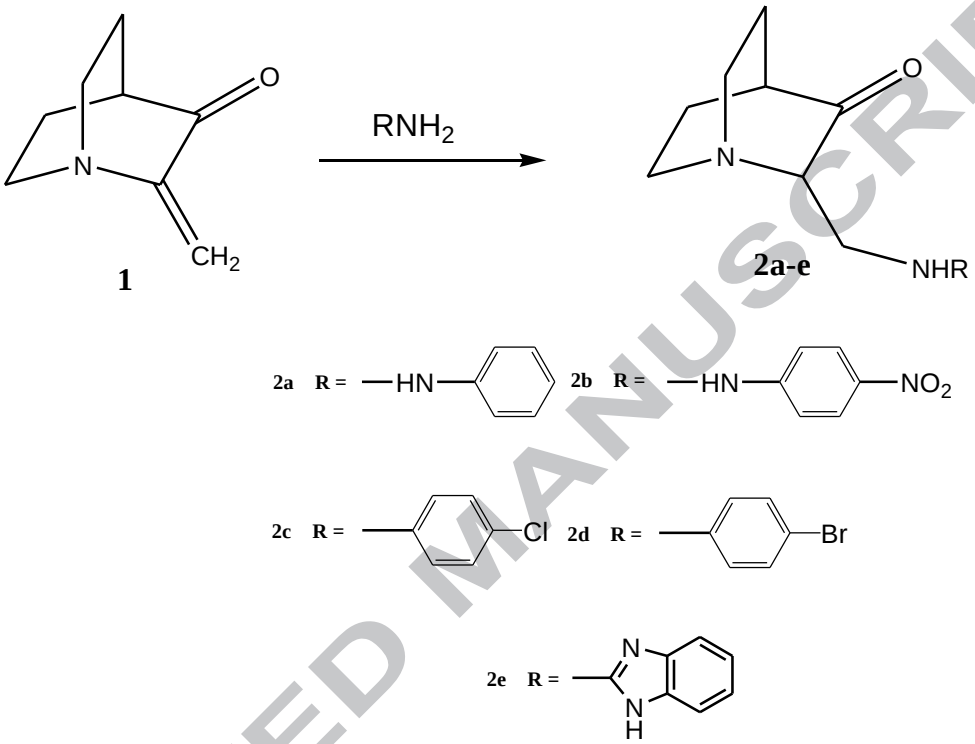

Scheme 1

Figure captions

Fig. 1 structures of some quinuclidine based drugs.

Fig. 2 Impact of derivative 2e on proliferation and apoptosis in breast cancer cells. Cell proliferation assay was performed to detect living cells. MCF-7 cells were treated with 10 µM of 2e for 24 h (A). Dose response curve was done to determine the IC50 for the potent derivative 2e (B). Cell viability was determined for both MCF-7 cells and MCF-12 by using 4 µM of derivative 2e (C). Determination of apoptosis in MCF-7 cells and MCF-12 cells by 4 µM 2e and 24 h duration interval (D). Each data point is the mean of three independent experiments and expressed as M±SD. Induction of apoptosis represents absorbance at 405 nm. TUNEL assay was used to confirm induction of apoptosis between treated and non-treated cells. MCF-7 cells were treated with 4 µM 2e for 24 h and induction of apoptosis was confirmed by appearance of TUNEL positive cells (E). Cell proliferation assay was performed to detect living cells. MDA-MB-231 were treated with 4 µM of 2e for 24 h (F). Apoptosis was determined in MDA-MB-231 cells by 4 µM 2e and 24 h duration interval (G)

Fig. 3 Derivative 2e reduced cells in G2/M checkpoint in MCF-7. The % of cell cycle phases was determined in MCF-7 cells after treatment with 4 µM drugs of drug 2e for 24 h (A). Cells were treated with derivative 2e, total protein was extracted and used for Western blotting analysis to determine the differences in cyclin D and cyclin B expression levels between treated and non-treated cells at the same condition (B). β-actin was used as loading control protein

Fig.4 Inhibition of p53 signaling by derivative 2e. MCF-7 Cells were treated with derivative 2e, total protein was extracted and used for Western blotting analysis to determine the differences in Mdm2, p53, Akt and ERk1/2 expression levels between treated and non-treated cells at the same condition (A). β-actin was used also adding control protein. MCF-7 cells were with 10 µM PFT-α for 1 hr and then treated with 100 µM derivative 2e for additional 24 hrs and cells then harvested to extract same proteins mention under same condition (B). induction of apoptosis was determined as indicated by reading Abs at 405 nm for control, treated cells with derivative 2e and cells treated with both derivative 2e and 10 µM PFT-α. Each data point is the mean of three independent experiments and expressed as M±SD. induction of apoptosis was determined as indicated by reading Abs at 405 nm for control, treated cells with derivative 2e and cells treated with both derivative 2e and 15 µM PFT-α. Each data point is the mean of three independent experiments and expressed as M±SD

Fig. 5. Binding mode of lead fragment in the mutation-induced cavity of T-p53C-Y220C using MOE software

Fig. 6. Binding mode of compound 2e docked and minimized in the mutation-induced cavity of T-p53C-Y220C using MOE software

Novel Quinuclidinone Derivatives Induced Apoptosis in Human Breast Cancer *via* Targeting P53

Ahmed Malki , Rasha Y. Elbayaa , Omnia Ali, Ahmed Sultan, Amal M. Youssef

The present work describes the design and synthesis of novel series of five quinuclidinone derivatives **(2a-2e)**.Their anticancer activities were investigated against breast cancer cells MCF-7, MDA-MB-231 breast cancer cells harboring mutant p53 and normal breast counterpart MCF-12a. Derivative **2e** reduced proliferation of MCF-7 and MCD-12a while it has no effect on MDA-MB-231.Derivative **2e** induced apoptosis in MCF-7 cells which is further confirmed by TUNEL assay and it reduced the percentage of cell in G2/M phase as confirmed by increased expression of cyclin B and reduced expression of cyclinD1.Derivative **2e** reduced expression levels of Mdm2, Akt and ERK1/2 by and increased expression

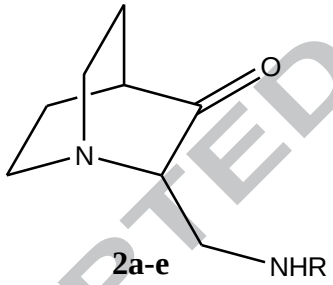

2a-e